D'Amario L, Jiang R, Cappel U, Gibson E, Boschloo G, Rensmo H, Sun L, Hammarström L, Tian H.

Chemical and Physical Reduction of High Valence Ni States in Mesoporous NiO Film for Solar Cell Application.

***ACS Applied Materials and Interfaces* 2017**

DOI: https://doi.org/10.1021/acsami.7b01532

Chemical and Physical Reduction of High Valence Ni States in Mesoporous NiO Film for Solar Cell Application.

Luca D'Amario,[†] Roger Jiang,[†] Ute Cappel,[‡] Elizabeth A. Gibbson,[¶] Gerrit Boschloo,[†,§] Håkan Rensmo,[‡] Licheng Sun,[∥,§] Leif Hammarström,[*,†] and Haining Tian[*,†,§]

Department of Chemistry - Ångström Laboratory, Uppsala University, Box 523, 751 20 Uppsala, Sweden,
Department of Physics and Astronomy - Ångström Laboratory, Uppsala University, Box 516, 751 20 Uppsala, Sweden,
School of Chemistry, Newcastle University, Newcastle upon Tyne, NE1 7RU, U.K.,
Center of Molecular Devices, Department of Chemistry, Royal Institute of Technology (KTH), 10044 Stockholm, Sweden, and
Department of Chemistry, Organic Chemistry Royal Institute of Technology (KTH), 10044 Stockholm, Sweden

E-mail: leif.hammarstrom@kemi.uu.se; haining.tian@kemi.uu.se
Phone: +46 (0)18 471 3648; +46 (0)18 471 3638. Fax: +46 (0)18 471 6844

Abstract

The need of a p-type semiconductor for a working dye sensitized tandem solar cell drives the research on NiO mesoporous films. In this paper we achieved to make the usual brownish NiO more transparent by reducing Ni^{3+} impurities. Two pretreatment methods have been used: chemical reduction by $NaBH_4$ and thermal reduction by heating. The power conversion efficiency of the cell has been increased 50% through chemical treatment and an improvement over 100% has been obtained for the open-circuit voltage upon heat treatment. We suggest that the reduction of surface Ni^{3+} (and Ni^{4+}) to Ni^{2+} decreases the recombination reaction between holes on the NiO surface with the electrolyte. It also keeps the dye firm on the surface building a barrier for electrolyte recombination. This caused an increase in open-circuit photovoltage from 105 mV for the untreated film to 225 mV for the treated film.

Introduction

In recent years, increasing attention is being paid to p-type dye-sensitized solar cells (p-DSCs) for the conversion of solar energy to electricity or fuels.[1–8] The aim of developing p-DSCs is to combine them with n-type DSCs (n-DSCs) in order to fabricate tandem solar cells to produce a higher conversion efficiency than the individual solar cell.[1,6,9] Theoretically, in the case of photovoltaic devices, the efficiency of tandem solar cells is expected to significantly exceed that of the individual cells and to overcome the Shockley-Queisser limit.

[*]To whom correspondence should be addressed
[†]Department of Chemistry - Ångström Laboratory
[‡]Department of Physics and Astronomy - Ångström Laboratory
[¶]School of Chemistry, Newcastle University
[§]Center of Molecular Devices, KTH
[∥]Department of Chemistry, Organic Chemistry, KTH

So far, no tandem cells have achieved an efficiency exceeding state-of-the-art n-DSCs because they are limited by the poor performance of the p-type photoelectrode (record of photoconversion efficiency 2%).[10] Therefore, further development of p-DSCs is desirable. In p-DSCs, a mesoporous NiO film is typically employed as p-type semiconductor material which transports the holes, injected from a photosensitizer, to the conducting substrate.[11] The preparation method for the NiO films significantly impacts the performance of the device.[12,13] The most success has been reached using the method reported by Suzuki and co-workers which uses a precursor solution of $NiCl_2$, and a triblock copolymer (F108) in water and ethanol to prepare the nano NiO film.[14,15] By using this procedure in combination with an efficient "push-pull" photosensitizer, a record IPCE value of 64% was achieved.[15] However, as it is typically the case for nanostructured NiO, we found that the NiO film was not transparent, which is due to the existence of Ni^{3+} in the film.[16] Ni(III) is present as a result of Ni(II) vacancies in the material, which is thought to be responsible for the p-type character of NiO, which otherwise would be a Mott-insulator.[17] Previously, we have suggested that the charge transport mechanism in NiO films may occur by hole hopping at the surface of the nanocrystals.[18] However, the presence of excess Ni^{3+} at the surface of the film may be responsible for the high rate of recombination between the reduced dye and holes in the NiO observed with organic photosensitizers.[19–24] Therefore we have attempted to reduce the amount of Ni^{3+} in the NiO film. We reduced the amount of Ni^{3+} by both a chemical and a thermal method. The chemical method, which involved immersing the NiO electrodes in an acetonitrile solution of $NaBH_4$ was successful in reducing the amount of Ni^{3+}. The thermal method was simply performed by heating the NiO films on FTO in the oven at 200°C for 2 minutes. The p-DSC cells built with the reduced NiO film showed an unexpected improvement in photovoltaic performance in comparison to the ones made with the untreated films, especially in terms of photovoltage.

Results and Discussion

Figure 1 shows the transmittance spectra of NiO films (without dye) which have been subjected to the mentioned treatments. As anticipated, soaking the NiO electrodes in a 0.1 M $NaBH_4$ in acetonitrile solution for five minutes greatly improved the transmittance of the film ($NiO/NaBH_4$ sample). The improvement in transmittance was ascribed to the reduction of Ni^{3+} to Ni^{2+} . To check the effect of a base solution on the NiO transmittance, another electrode was immersed in a saturated acetonitrile solution of t-BuONa for five minutes (NiO/t-BuNa sample). This was found to improve the transmittance slightly, possibly due to some exchange of protons on the electrode surface with sodium (confirmed by XPS measurements, SI).

The same effect on the transmittance is obtained by heat-treatment (NiO/heated sample). This effect is again attributed to the reduction of Ni^{3+} content in the nanoparticles.

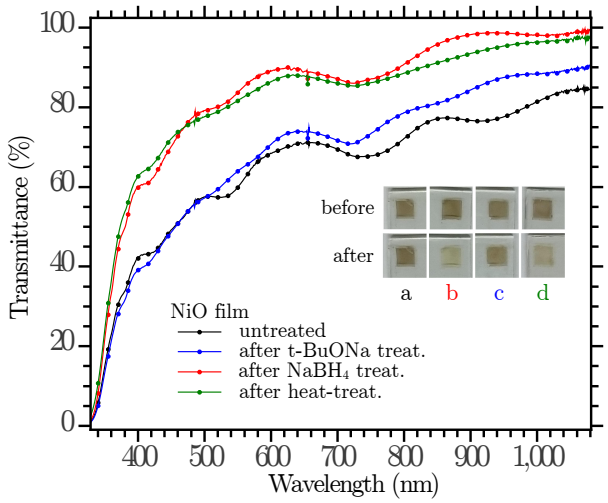

Figure 1: Transmittance of NiO films on FTO treated with the variuos methods. The baseline of the transmittance spectrum was taken with a clean FTO glass. The black trace (**a** pct) corresponds to the untreated NiO film; the red trace (**b** pct) to the $NiO/NaBH_4$ film; the blue one (**c** pct) to the NiO/t-BuNa film and the green trace (**d** pct) to the NiO/heated sample.

To compare the effects of the treatments on dye adsorption the films were immersed in an

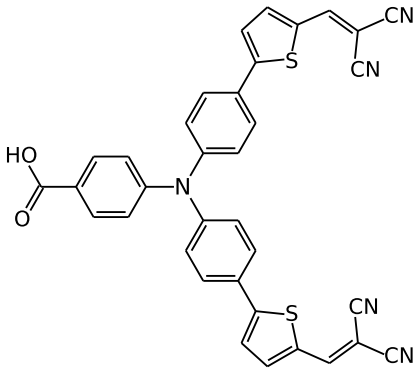

Figure 2: Molecular structure of the **P1** dye.[25]

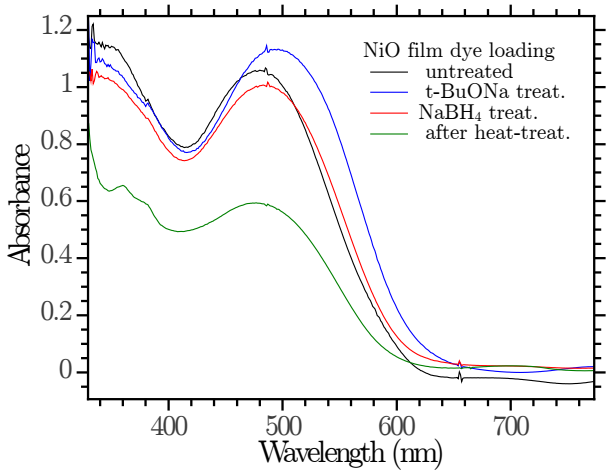

Figure 3: Absorbance of the **P1** -sensitized NiO films prepared with the different methods. The color code is the same as in Figure 1. The spectra were recorded using air as baseline, the absorption of the FTO glass and the unsensitized film, of each treatment, were subtracted afterwards.

acetonitrile solution of the **P1** dye overnight. **P1** , see Figure 2, is a standard dye well characterized for p-type DSC.[13,25,26]

Figure 3 reports the absorption spectra of the sensitized films and shows how the chemical treatments, $NaBH_4$ and t-BuONa, did not significantly affect the adsorption of dye molecules. The spectra look quite similar, with a small red shift of the NiO/$NaBH_4$ and NiO/t-BuNa samples. Contrarily to the chemical treatments the physical treatment is affected by a significant lower dye loading, see the green trace in Figure 3. This is due to a modified hydrophilicity of the surface, discussed later in this paper.

Solar cell characterization

The sensitized electrodes were used to assemble p-DSCs with a platinized counter electrode and LiI/I_2 as RedOx couple in acetonitrile electrolyte. The photocurrent density-photovoltage (J-V) curves of the p-DSCs containing the different NiO films are shown in Figure 4 and the corresponding solar cell parameters are collected in Table 1.

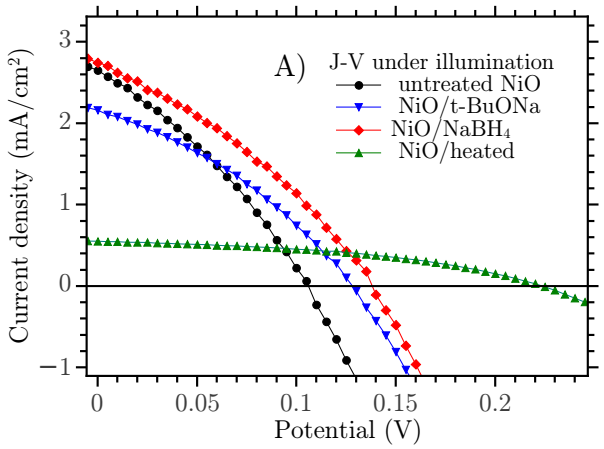

(a) Under illumination

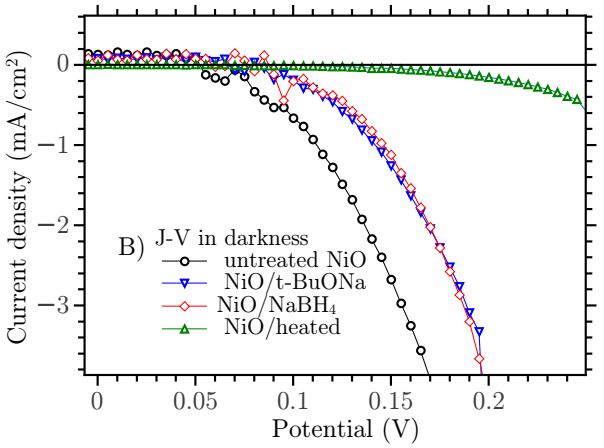

(b) In darkness

Figure 4: Current density vs. applied potential of the p-DSSC prepared with the film variously treated: Figure **a** under illumination; Figure **b** in darkness. The experimental details are given in Table 1.

Table 1: The photovoltaic properties of p-DSCs based on different NiO films.[a] Errors in RSD are given in the squared bracket.

Film[b]	Jsc (mA/cm^2)	Voc (mV)	FF	μ (%)
NiO	2.6 [2%]	105 [2%]	0.32	0.09 [3%]
NiO/t-BuNa	2.1 [3%]	130 [5%]	0.34	0.09 [6%]
NiO/$NaBH_4$	2.7 [4%]	140 [4%]	0.32	0.12 [6%]
NiO/heated	0.55 [9%]	225 [7%]	0.42	0.05 [12%]

a-light intensity: AM 1.5 G, 100 mW/cm^2; electrolyte: 1 M LiI and 0.1 M I_2 in MeCN

b-active area of film: 0.25 cm^{-2}; film thickness: 1.4 μm.

Whilst there was a noticeable improvement in fill factor (FF) for the NiO/heated p-DSC, the significant differences among the devices were in the open-circuit potential (Voc) and short-circuit current (Jsc). The Voc improved from 105 mV for the untreated film, to 130 mV for the NiO/t-BuNa film, to 140 mV for the NiO/$NaBH_4$ film and to 225 mV for the NiO/heated film. The Jsc instead improved in the NiO/$NaBH_4$ case but drastically decreased for NiO/heated. It is clear that in the case of the NiO/$NaBH_4$ p-DSC the photovoltage is the key of the higher performance, for the contrary the cause of bad performance of the NiO/heated p-DSCs is the poor current, see Figure 4a. In fact the NiO/heated films preformed only with a 0.05% efficiency compared with the untreated NiO-based device which operated with an efficiency of 0.09%. Instead, as said, the p-DSC containing the NiO/$NaBH_4$ electrode operated with a much higher efficiency of 0.12%. Compared with the untreated NiO, the p-DSC containing NiO/t-BuNa operated with the same efficiency. The dark current experiment, reported in Figure 4b, agrees with the observation regarding the Voc. The untreated film shows the higher dark current with an onset potential around 70 mV, the $NaBH_4$ and the t-BuONa treated DSC show the same behaviour with the onset potential at 100 mV while the heat treated film shows the lowest current for the entire range of measure with the onset potential at around 170 mV.

The photoelectrochemical properties of the p-DSCs were compared using photocurrent and photovoltage decay experiments to explore the cause of the different Voc and Jsc values obtained. Recall that in DSCs the Voc is determined by the potential difference between the quasi-Fermi level (E_F^q) of the semiconductor and the RedOx couple in the electrolyte. The E_F^q depends on both the position and the concentration of holes in the NiO valence band/trap states, while the RedOx couple potential depends on the concentration of the species. Figure 5a is a plot of the extracted charge vs. the open-circuit potential of the p-DSCs. The NiO/$NaBH_4$ and NiO/t-BuNa samples have practically the same behaviour. The amount of charges extracted from the untreated, NiO/$NaBH_4$ and NiO/t-BuNa samples are in the same order of magnitude. It is observed that at the same charge value there is a substantial difference in Voc (38 mV) from the untreated and the two chemically treated DSCs, which can be addressed to a different E_F^q position respect to the redox couple potential. The NiO/heated p-DSC shows a much lower charge volume (one order in magnitude less). It is excluded that this small amount of extracted charges is due to a poor injection derived from the aforementioned small dye loading in the heated sample. In fact this is only the half of the other samples and it cannot explain a decrement of an order in magnitude of extracted charges. Instead, this large difference can be attributed to the more effective insulation layer built by the dye on the NiO surface caused by a different binding mode. This effect is supported by contact angle measurement, vide infra.

The hole lifetimes (τ_h) in the p-DSCs constructed with the different films were determined from the photovoltage decay at open circuit and are plotted as a function of Voc in Figure 5b. τ_h of the NiO/$NaBH_4$ and NiO/t-BuNa films was similar each other and higher than the untreated one, about the double at the same Voc. For the NiO/heated case τ_h is considerably longer. Generally, a longer lifetime can be assigned to a decreased recombination, which leads to an increased Voc, which is observed.

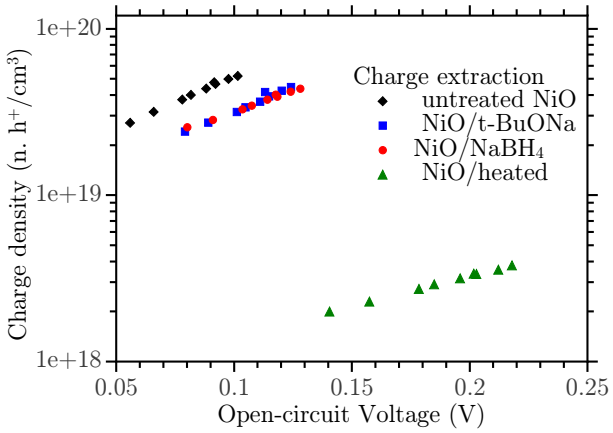

(a) Charge extraction.

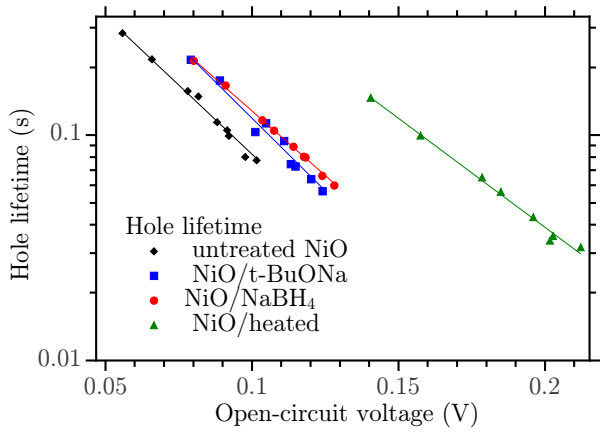

(b) Hole lifetime.

Figure 5: Hole lifetime and charge extraction measurement of the p-DSCs. In the hole extraction measurement the light intensity is ranged from 0.1 to 2 suns. In the hole lifetime the intensity is 1 sun.

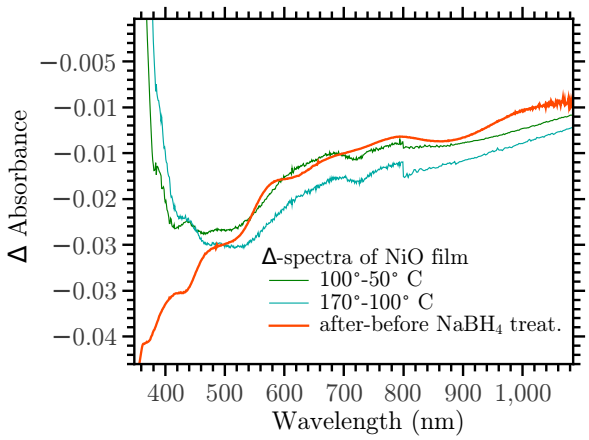

Figure 6: Absorption differences, after treatment - before treatment, of NiO film sintered on CaF_2. The Δ-spectra of the absorption recorded at two temperatures are given in green and the cyan (T are reported in the Figure). The orange curve is the Δ-spectra upon $NaBH_4$ treatement.

Film characterization

Since the main effect of the treatments was the change in transmittance of the samples, see Figure 1, we looked at the spectral differences before and after the processes to understand the effects in the semiconductor. The spectral differences (Δ-spectra) obtained upon each treatment are plotted in Figure 6.

The Δ-spectra associated with the heat treatment samples are recorded after annealing at two different temperatures (100°-50° and 170°-100° C, respectively the green and cyan Δ-spectra). The 100°-50°C Δ-spectrum is reported to show that the reaction is active already at small temperatures. The three bleaches are quite similar in the visible range while differ substantially in the UV: the absorption from the $NiO/NaBH_4$ sample (orange spectrum) decreases even in the UV in contrast to the bleaches of the NiO/heated samples.

To be able to characterize the specific effect of the treatments on the composition of the NiO nanoparticles we performed spectro-electro-chemistry (SEC) of a bare NiO film on FTO glass in acetonitrile, the result is plotted in Figure 7. This spectro-electro-chemistry is quite similar to the one previously recorded in water by Boschloo.[16] The spectra were collected each 100 mV ranging from -400 mV to 500 mV (vs. Ag/Ag^+). The spectrum recorded at -400 was used as baseline. As previously reported, the spectral features are a broad absorption band at 350-500 nm on top of a structureless broad absorption covering the entire visible range. The spectrum shape changes slightly as the potential is ranged from -400 mV to 500 mV. The absorption increases with the potential, see the arrow. Though the difference in absorption between two potential steps it is not uniform through the potential range. In other words the differential of the absorp-

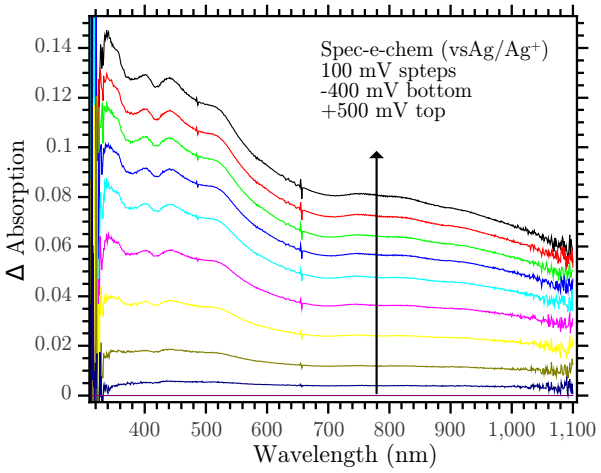

Figure 7: SEC spectra of untreated NiO on FTO recorded each 100 mV from -400 to 500 mV vs. Ag/Ag^+. $LiClO_4$ 0.5 M in MeCN was used as electrolyte.

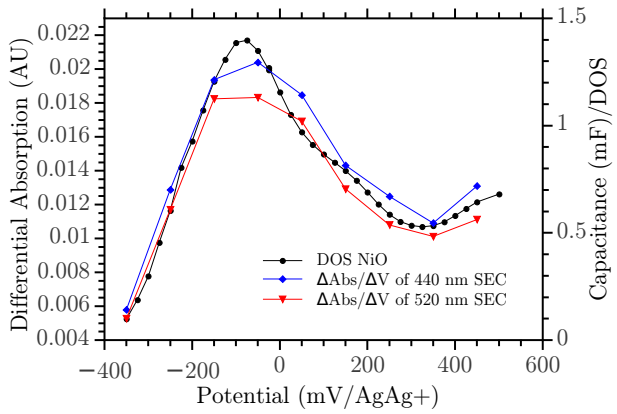

Figure 8: $\Delta Abs/\Delta V$ of the 440 nm and 520 nm wavelength of the SEC in Figure 7 vs. the potential, blue and red respectively. In black the DOS (by capacitance) reported from D'Amario et al.[27]

tion (dAbs/dV) is not constant with the potential variation. This might be related to the not constant first derivative of NiO density-of-states (DOS) respect to the potential in this interval of voltages. For comparison, in Figure 8 one can see the $\Delta Abs/\Delta V$ of two wavelengths of the SEC and the DOS of mesoporous NiO vs. the applied potential. It is clear that the differential of the absorption follows the DOS.

By comparison of electro-chemistry and XPS data reported in literature by Dini et al.[28] the

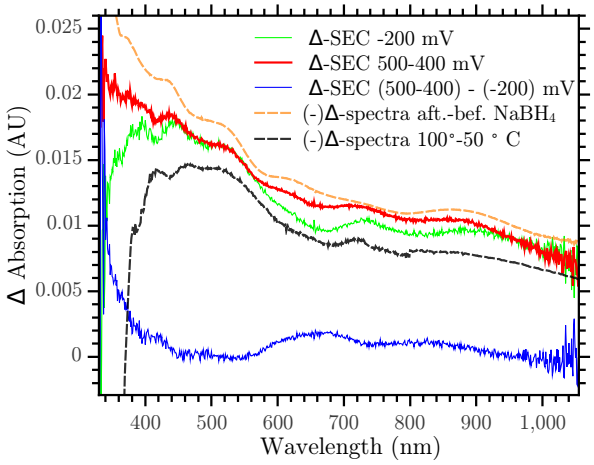

Figure 9: Δ-SEC (solid line) extracted from SEC and comparison with the (-)Δ-spectra of Figure 6 (dashed line).

peaks of the DOS can be assigned to the various oxidation states of Ni. Dini et al. found on NiO surface the presence of only Ni^{2+}, Ni^{3+} and Ni^{4+}. Because of this we have not considered other oxidation states, like Ni^0 found in one other source.[29] The comparison of electrochemistry and XPS reveals that the pronounced peak at -100 mV is due to the oxidation of Ni^{2+} to Ni^{3+} and the peak that starts appearing at 450 mV results from the oxidation of Ni^{3+} to Ni^{4+}. The fact that the SEC correlate so well with the DOS gives the possibility to extract the specific spectra of each peak of the DOS, i.e. of each redox state. These spectra (Δ-SEC) are reported in Figure 9. The green trace is the spectrum recorded at -200 mV, where Ni^{2+} oxidation occurs. This Δ-SEC is thus assigned to Ni^{3+} . The red trace is the spectrum recorded at 500 mV minus the one recorded at 400 mV: 400-500 mV is the range where Ni^{4+} appears in the DOS. Finally the blue trace is the difference between these last two, red - green. The subtraction is made to remove possible spectral components due to the oxidation of Ni^{2+} to Ni^{3+} that can still occur at these potentials. Thus we attribute the blue Δ-SEC to Ni^{4+}. This is an important finding since it is the first time that a UV-Vis spectrum can be assigned to a specific oxidation state of Ni of a NiO nanoparticle.

These characteristic spectra extracted from SEC can be helpful in understanding the bleaches discussed previously, after the various film treatments (Figure 6). In Figure 9, the absorption of the Δ-spectra from Figure 6 are displayed in orange and black. One can see that the Δ-spectrum due to the $NaBH_4$ treatment (orange) resembles the spectrum which was attributed to a mixture of Ni^{2+} and Ni^{3+} absorptions (red). Instead the bleaching due to the heat treatment (black) resembles the Ni^{3+} Δ-SEC (green). [1]

We have now the spectral evidence that the bleaching caused by the two treatments are depleting the Ni^{3+} (and Ni^{4+} in the case of $NaBH_4$) from the nanoparticles. It is quite straightforward to explain this effect in the case of the $NaBH_4$ treatment. Ni^{3+} in NiO nanoparticle can be found as Ni_2O_3 and as NiOOH sites and Ni^{4+} as NiO_2. $NaBH_4$ is a source of H^- that can reduce the Ni^{3+} and Ni^{4+} by the following reactions:

$$NiOOH + H^- \longrightarrow NiO + H_2O + e^- \quad (1)$$

$$Ni_2O_3 + 2H^- \longrightarrow 2NiO + H_2O + 2e^- \quad (2)$$

$$NiO_2 + H^- \longrightarrow NiO + OH^- \quad (3)$$

The electrons released from the hydride will reduce Ni-sites in NiO and the charge neutrality is conserved by Na^+ ions that might be adsorbed on the surface and/or by lattice modification. The mechanism proposed here might be simplistic because it only considers Ni^{3+} as the two oxides, while it can be in found in a defect of the crystal in many (unknown) forms. In any case the reduction will occur by the oxygen and the hydride.

The explanation of how Ni^{3+} impurities are removed from NiO nanoparticles simply by heat is done by considering the reversibility of the reduction process. In fact after the bleaching upon heat treatment the NiO film comes back to its former color in 3-4 h if kept under air or oxygen, see Figure S1 in SI. On the contrary the reversibility is blocked if the heating is conduced under inert atmosphere, see Figure S1c. It is clear that oxygen plays a key role in the reversibility of the Ni^{3+} reduction. This is explained by hypothesizing that NiO, Ni_2O_3 and NiOOH have close formation energies so that they are in equilibrium with each other. This would make the decomposition of the high valence oxides into NiO easily driven by temperature.

The formation reaction of Ni_2O_3 from NiO is:

$$2\ NiO(s) + 1/2\ O_2(g) \longrightarrow\ Ni_2O_3\ (s)$$

If NiO and Ni_2O_3 are close in formation enthalpy then the balance of this reaction is driven by entropy, thus by temperature, due to O_2 in gas form.

The same mechanism is considered for NiOOH, which equilibrium reaction with NiO is:

$$2NiOOH(s) \overset{\text{heat}}{\rightleftharpoons} 2NiO(s) + \tfrac{1}{2}O_2(g) + H_2O(g)$$

Also this reaction can be driven by temperature especially above 100°C where H_2O is in gas form.

The last confirmation of the occurrence of high valence Ni reduction comes from XPS analysis of the films. Unfortunately the resolution of our experiment was not enough to give a direct evidence of the valence changes of Ni occurring on the surface. However we were able to see a remarkable shift of the valence band respect to the Fermi level, related to the Ni ion reduction. The result of the VB signal vs. Fermi level is plotted in Figure 10.

All the samples show the same shape the only difference is a shift respect to Fermi level. The shift is due to the reduction of the high valence Ni states in the NiO nanoparticle. For this reason the results are considered as a Fermi level upwards shift rather than a VB potential movement. The NiO/t-BuNa sample and the reference (untreated) NiO lies in the same position, thus no shift of the Fermi level, as it was expected. The $NiO/NaBH_4$ sample shows

[1] The small differences between the Δ-spectra and the SEC might be due to the fact that the first ones are collected with dry films while the SEC are in electrolyte.

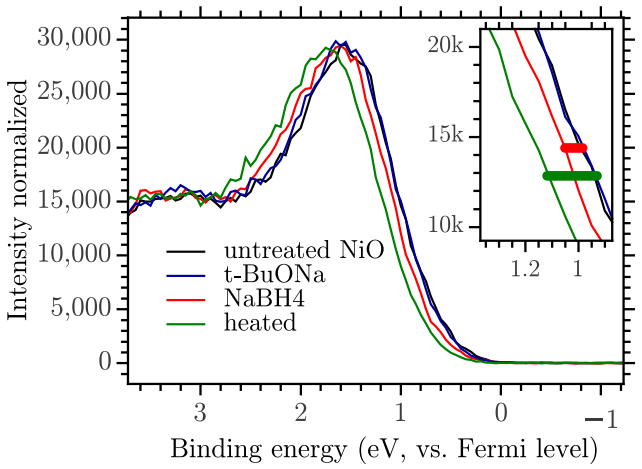

Figure 10: Valence spectra of the different NiO samples calibrated against the Fermi level of an external Au reference. Inset: enlargment of the Valence Band edge shift, the red bar correspond to 80 meV while the green to 220 meV.

a displacement of 80 meV (±50 meV), while the NiO/heated sample shifts 220 meV (±50 meV). This confirms the efficacy of the reduction treatments and suggest that the physical treatment is more effective than the chemical one.

XPS data also confirm that only the two chemical treatments substitute protons on the NiO surface with sodium ion which are clearly visible in the Na[1s] spectra (see supporting material).

Explanation of solar cell data

It is now clear that the $NaBH_4$ treatment and heat treatment reduce the amount of high-valence Ni states on the surface of the nanoparticles. Furthermore one has to remember that all three methods reduce the content of water and proton from NiO surface substituting H^+ with Na^+ when necessary. A summary of the changes that each treatment causes to the NiO surface is sketched in Figure 11. In the following section we suggest a model to explain how the aforementioned surface modification result in the p-DSC performances presented at the beginning of the paper.

All the treatments are able to increase the Voc, lower dark current and prolong the hole lifetime respect to the reference. These are common signs of reduced electrolyte recombination. In this case this could be due to two main reasons: a reduced amount of recombination paths caused by a lower Ni^{3+} content; and a better coverage of the surface due to a different binding of the dye to the NiO. In untreated NiO the surface Ni^{3+} sites work as funnels for recombination by trapping the injected holes as Ni^{4+}. This highly energetic state reacts quickly with the reduced state of the dye or with the reduced RedOx shuttle. It has been proposed by Boschloo et al. that the injected holes are neutralized by proton expulsion from a NiOOH site.[16] This makes the hole-traps exposed to the Redox couple speeding up the recombination. The pool of high energy traps is then quickly emptied rising up the quasi-Fermi level (E_F^q) towards the low energetic Ni^{3+} traps. As a consequence of this the Voc is reduced, see Figure 12 a. In the NiO/$NaBH_4$ case the Ni^{3+} sites are substituted with Ni^{2+} sites with or without a Na^+ counter-ion, see Figure 11. The low Ni^{3+} content blocks the possibility of trapping the hole by Ni^{4+}, thus the holes can accumulate deeper in the DOS pushing the E_F^q to positive values, see Figure 12 b. Furthermore, the lower Ni^{3+} content makes the dye bind stronger to the surface, as seen from dye dye electrochemical-desorption measurement (see supporting material for further details). These two effects both contribute to improve the Voc and increase the hole lifetime. Moreover the fact that the surface still hosts ions that can neutralize the trapped hole by ion expulsion keeps a high amount extracted charges. The NiO/t-BuNa p-DSC show a behaviour in between the untreated and NiO/$NaBH_4$. This could be due to a mix of factors like better dye loading, ion exchange by proton removal. The case of the heat treated film is different. In fact in this case we notice a much higher Voc, decreased extracted charges, lower dye loading and lower short-circuit photocurrent. The physical heat reduction reduces the Ni^{3+} amount without support of any counter-ion and it reduces the water content. Both of these facts might be relevant for the dye loading. We propose that the **P1** com-

pletely changes the binding mode such that the dye occupies more space on the surface (thus less dye loading) and offers a better barrier for electron transfer. Probably the dye lies on the surface instead of standing up perpendicular to it. This is supported by contact angle measurement of water on the heated film respect to normal NiO. The heated surface is more hydrophobic than the normal one with a contact angle of 53° respect to 29° of the untreated surface, see supporting material. Thus, it is possible that the dye is covering so well the surface that the possibilities of stabilizing the trapped holes are very low. Trapping by Ni^{3+} or Ni^{4+} is suppressed, see Figure 12 c. Without the support of traps, the injected holes need to accumulate in the valence band adopting an exponential filling of the states. This results in a more positive E_F^q, thus higher Voc, but in much less extracted charges since the recombination with the reduced dye would be much quicker. A fact that supports this hypothesis is the variation of the Voc respect to the illumination intensity in the charge extraction experiment, see Figure 5a. In that measurement the light intensity is ranged from 0.1 sun to 2 suns, the Voc of all the samples range 50 mV except for the NiO/heated Voc that ranges 80 mV. In other words the charge extraction curve of the NiO/heated sample is less steep. The larger variation of the Voc upon intensity change supports the hypothesis of reduced trapping in the heated sample.

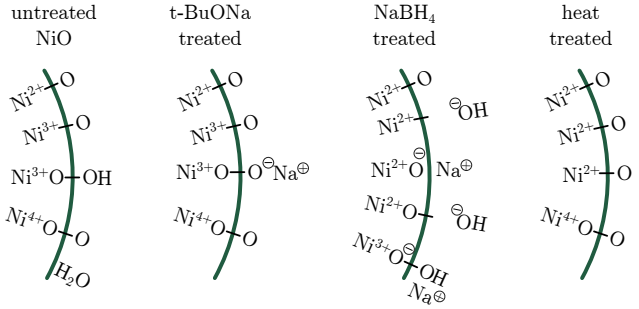

Figure 11: Summary of the effects of the different treatment to the composition of NiO surface.

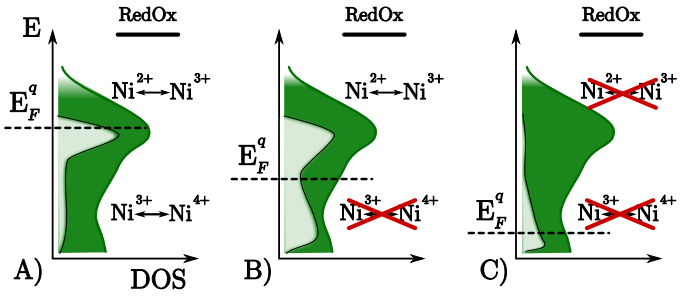

Figure 12: Schematization of the hole distribution vs. the potential in the three different films respectively from left: untreated NiO, $NiO/NaBH_4$, NiO/t-BuONa. The DOS of NiO is represented with the dark green area (real data from DOS, see Figure 8). The white-green area represents the hole distribution (not real data, it is a qualitative schematization). The potential of the RedOx couple is placed as a reference to indicate the effect in the Voc.

Conclusion

In summary, two effective methods, chemical reduction with $NaBH_4$ and physical reduction by heating, was adopted to treat the NiO film in order to diminish the slight amount of high valence Ni ion in the film. Both of the methods greatly improved the transmittance of the films. The **P1** dye-based p-DSCs fabricated by the chemically treated NiO film ($NiO/NaBH_4$) rendered a higher Voc value 140 mV comparing with the normal NiO film that gave a 105 mV Voc value. The physically treated had even a higher Voc of 225 mV. The species reduced by chemical and physical methods were characterized by spectro-electro-chemistry and distinctively different UV-Vis spectra were assigned to Ni^{3+} and Ni^{4+} states, respectively. Physical reduction was explained by decomposition of NiOOH to oxygen and water. Photoelectrochemical measurements proved that the proton and sodium ions present on the untreated and chemically treated p-DSC were essential for a high photocurrent providing hole-trap stabilization and thus high charge accumulation. The heat treatment removes the majority of the free ions from the NiO surface resulting in no trap stabilization. It was found to be the essential

factor for the best Voc, it allowed a different dye adsorption that prevented recombination and pushed down the quasi Fermi level by avoiding the filling of the surface traps. The result suggests that the dynamics of the ion on the surface of NiO is more complex than thought. Tuning the ion content and composition of the NiO surface shows a significant effect on the performance of p-DSCs and should be critically considered in the future research.

Experiments

General

UV-Vis absorption was recorded on an Agilent 8453 UV-vis spectrophotometer for all the samples except for the spectra recorded at high temperature when a Varian Cary 5000 spectrophotometer was used. J-V characteristics were measured using a Keithley source/meter under simulated sunlight from a Newport 300 W solar simulator, giving light with an intensity of 100 mW/cm2. Both systems were calibrated against a certified reference solar cell (IR-filtered, silicon solar cell, Fraunhofer ISE, Freiburg, Germany). The active area of the DSCs studied was 5 mm x 5 mm. A black mask (6 mm x 6 mm) was used in the photovoltaic measurements. All chemicals were ordered by Sigma-Aldrich and used as received.

XPS measurement

XPS measurements were performed with a Scienta ESCA 300 using monochromatized AlKα radiation (photon energy = 1486.7 eV). Spectra were measured in normal emission (90°) and the pressure in the analysis chamber was approximately 1e10-8 mbar. The mean free path (λ) of electrons emitted from the Ni[2p] level is approximately 1 nm at this energy and take off angle giving a probing depth (3λ, 90% of electrons) is 3 nm. The spectra were energy calibrated versus the Fermi level using an external gold electrode and setting the energy of Au[4f] to 84.0 eV. Core level spectra were then further more shifted to match the Ni[2p] position of the untreated reference sample for ease of comparison. A shift of -0.22 eV was applied to spectra of the NiO/heated sample and a shift of -0.08 eV to the $NaBH_4$ treated sample. Core level spectra were intensity normalised to area of the Ni[2p] spectrum for each sample.

Photoelectrochemical Measurements

Hole lifetimes for the solar cells were estimated using a white-light-emitting diode (Luxeon, 1 W) as the light source. Voltage and current traces were recorded by a 16-bit resolution data acquisition board (DAQ National Instruments) in combination with a current amplifier (Stanford Research SR570). The relation between potential and charge was studied using a combined voltage decay/charge extraction method. Charge extraction measurements were carried out as follows: the solar cell was illuminated for 5 s under open-circuit conditions, and then the light was switched off and the voltage was allowed to decay to a voltage V. At a certain voltage V, the cell was short-circuited, and the current was determined under 10 s and then integrated to obtain the charge, Qoc (V). Hole lifetimes was determined by monitoring the photovoltage response after a small perturbation (1 %) of the light intensity.

Preparation of Counter Electrodes

Platinized, fluorine-doped, tin oxide (FTO) conducting glass counter electrodes (CEs) were prepared by sintering H_2PtCl_6 isopropanol solution uniformly distributed on the surface of the FTO substrates (5μL/cm^2, 1 M solution).

p-DSC Fabrication

The two layers NiO films (1.2 μm thickness, area: 5 mm x 5 mm) were prepared through doctor-blading the $NiCl_2$ paste and were sintered under the atmosphere condition according to the previous method.[15] The chemical treated films were immersed into acetonitrile (MeCN), 0.1 M $NaBH_4$ MeCN solution and saturated t-BuONa MeCN solution for 5 min and then were

rinsed with pure MeCN to form the final semiconductor electrode, NiO/$NaBH_4$ and NiO/t-BuONa, respectively. The heat treated samples were prepared in the glovebox, heating the films on a hot plate for 2 min at 200°. The working electrodes (WEs) were obtained by sensitizing the different NiO films mentioned above into 0.2 mM **P1** MeCN for 2 h, and then were rinsed by MeCN. The platinized conducting glasses as counter electrodes (CEs) were sealed with WEs using 25 um Surlyn film through heating at 120°C. The electrolyte, 1 M LiI and 0.1 M I_2 in MeCN, were filled via the preparative hole on CEs. Finally, the holes were sealed by the Surlyn film and glass sheet to form our test p-DSCs.

Acknowledgement The authors are thankful to Dr. Lin Li and Dr. Peng Quin for discussions and the technical support. This work was founded by the Swedish Energy Agency and the K&A Wallenberg Fundation.

Supporting Information Available: Further material about procedure, method and characterization is available online as Supporting Information. This material is available free of charge via the Internet at `http://pubs.acs.org/`.

Author Information

Corresponding Author.

∗ Email: leif.hammarstrom@kemi.uu.se

∗ Address: Department of Chemistry - Ångström Laboratory, Uppsala University, Box 523, 751 20 Uppsala, Sweden

∗ Phone: +46 (0)18 471 3648

∗ Fax: +46 (0)18 471 6844

References

(1) Nattestad, A.; Perera, I.; Spiccia, L. Developments in and prospects for photocathodic and tandem dye-sensitized solar cells. *Journal of Photochemistry and Photobiology C: Photochemistry Reviews* **2016**, *28*, 44 – 71.

(2) Brennaman, M. K.; Dillon, R. J.; Alibabaei, L.; Gish, M. K.; Dares, C. J.; Ashford, D. L.; House, R. L.; Meyer, G. J.; Papanikolas, J. M.; Meyer, T. J. Finding the Way to Solar Fuels with Dye-Sensitized Photoelectrosynthesis Cells. *JOURNAL OF THE AMERICAN CHEMICAL SOCIETY* **2016**, *138*, 13085–13102.

(3) Odobel, F.; Le Pleux, L.; Pellegrin, Y.; Blart, E. New photovoltaic devices based on the sensitization of p-type semiconductors: challenges and opportunities. *Acc. Chem. Res.* **2010**, *43*, 1063–1071.

(4) Gibson, E. A.; Smeigh, A. L.; Le Pleux, L.; Fortage, J.; Boschloo, G.; Blart, E.; Pellegrin, Y.; Odobel, F.; Hagfeldt, A.; Hammarstrom, L. A p-type NiO-based dye-sensitized solar cell with an open-circuit voltage of 0.35 V. *Ang. Chem.-Int. Ed.* **2009**, *48*, 4402–4405.

(5) Chavhan, S. I.; Abellon, R. D.; van Breemen, A. J. J. M.; Koetse, M. M.; Sweelssen, J.; Savenije, T. J. Sensitization of p-type NiO using n-type conducting polymers. *J. Phys. Chem. C* **2010**, *114*, 19496–19502.

(6) He, J.; Lindstrom, H.; Hagfeldt, A.; Lindquist, S. Dye-sensitized nanostructured p-type nickel oxide film as a photocathode for a solar cell. *J. Phys. Chem. B* **1999**, *103*, 8940–8943.

(7) He, J.; Lindstrom, H.; Hagfeldt, A.; Lindquist, S. Dye-sensitized nanostructured tandem cell-first demonstrated cell with a dye-sensitized photocathode. *Sol. Energy Mater. Sol. Cells* **2000**, *62*, 265–273.

(8) Nattestad, A.; Mozer, A. J.; Fischer, M. K. R.; Cheng, Y. B.; Mishra, A.; Baeuerle, P.; Bach, U. Highly efficient photocathodes for dye-sensitized tandem solar cells. *Nat. Mat.* **2010**, *9*, 31–35.

(9) Nakabayashi, S.; Ohta, N.; Fujishima, A. Dye sensitization of synthetic p-type diamond electrode. *Phys. Chem. Chem. Phys.* **1999**, *1*, 3993–3997.

(10) Yu, Z.; Perera, I. R.; Daeneke, T.; Makuta, S.; Tachibana, Y.; Jasieniak, J. J.; Mishra, A.; Baeuerle, P.; Spiccia, L.; Bach, U. Indium tin oxide as a semiconductor material in efficient p-type dye-sensitized solar cells. *NPG ASIA MATERIALS* **2016**, *8*.

(11) Odobel, F.; Pellegrin, Y.; Gibson, E. A.; Hagfeldt, A.; Smeigh, A. L.; Hammarstrom, L. Recent advances and future directions to optimize the performances of p-type dye-sensitized solar cells. *Coord. Chem. Rev.* **2012**, *256*, 2414–2423.

(12) Dini, D.; Halpin, Y.; Vos, J. G.; Gibson, E. A. The influence of the preparation method of NiOx photocathodes on the efficiency of p-type dye-sensitized solar cells. *Coordination Chemistry Reviews* **2015**, *304305*, 179 – 201, COST: European Cooperation in Science and Technology Current Challenges in Supramolecular Artificial Photosynthesis.

(13) Wood, C. J. et al. A comprehensive comparison of dye-sensitized NiO photocathodes for solar energy conversion. *Phys. Chem. Chem. Phys.* **2016**, *18*, 10727–10738.

(14) Sumikura, S.; Mori, S.; Shimizu, S.; Usami, H.; Suzuki, E. Syntheses of NiO nanoporous films using nonionic triblock co-polymer templates and their application to photo-cathodes of p-type dye-sensitized solar cells. *Journal of Photochemistry and Photobiology A: Chemistry* **2008**, *199*, 1 – 7.

(15) Li, L.; Gibson, E. A.; Qin, P.; Boschloo, G.; Gorlov, M.; Hagfeldt, A.; Sun, L. Double-Layered NiO Photocathodes for p-Type DSSCs with Record IPCE. *Advanced Materials* **2010**, *22*, 1759–1762.

(16) Boschloo, G.; Hagfeldt, A. Spectroelectrochemistry of nanostructured NiO. *J. Phys. Chem. B* **2001**, *105*, 3039–3044.

(17) Biju, V.; Khadar, M. DC conductivity of consolidated nanoparticles of NiO. *Mater. Res. Bul.* **2001**, *36*, 21–33.

(18) Zhu, H.; Hagfeldt, A.; Boschloo, G. Photoelectrochemistry of mesoporous NiO electrodes in Iodide/Triiodide electrolytes. *J. Phys. Chem. C* **2007**, *111*, 17455–17458.

(19) Borgstrom, M.; Blart, E.; Boschloo, G.; Mukhtar, E.; Hagfeldt, A.; Hammarstrom, L.; Odobel, F. Sensitized hole injection of phosphorus porphyrin into NiO: Toward new photovoltaic devices. *J. Phys. Chem. B* **2005**, *109*, 22928–22934.

(20) Morandeira, A.; Boschloo, G.; Hagfeldt, A.; Hammarstrom, L. Photoinduced ultrafast dynamics of coumarin 343 sensitized p-type-nanostructured NiO films. *J. Phys. Chem. B* **2005**, *109*, 19403–19410.

(21) Zhang, L.; Favereau, L.; Farre, Y.; Mijangos, E.; Pellegrin, Y.; Blart, E.; Odobel, F.; Hammarstrom, L. Ultrafast and slow charge recombination dynamics of diketopyrrolopyrrole-NiO dye sensitized solar cells. *Phys. Chem. Chem. Phys.* **2016**, *18*, 18515–18527.

(22) Morandeira, A.; Boschloo, G.; Hagfeldt, A.; Hammarstrom, L. Coumarin 343-NiO films as nanostructured photocathodes in dye-sensitized solar cells: Ultrafast electron transfer, effect of the I-3(-)/I- redox couple and mechanism of photocurrent generation. *J. Phys. Chem. C* **2008**, *112*, 9530–9537.

(23) Flynn, C. J.; McCullough, S. M.; Li, L.; Donley, C. L.; Kanai, Y.; Cahoon, J. F. Passivation of Nickel Vacancy Defects in Nickel Oxide Solar Cells by Targeted Atomic Deposition of Boron. *JOURNAL OF PHYSICAL CHEMISTRY C* **2016**, *120*, 16568–16576.

(24) Flynn, C. J.; McCullough, S. M.; Oh, E.; Li, L.; Mercado, C. C.; Farnum, B. H.;

Li, W.; Donley, C. L.; You, W.; Nozik, A. J.; McBride, J. R.; Meyer, T. J.; Kanai, Y.; Cahoon, J. F. Site-Selective Passivation of Defects in NiO Solar Photocathodes by Targeted Atomic Deposition. *ACS APPLIED MATERIALS & INTERFACES* **2016**, *8*, 4754–4761.

(25) Qin, P.; Zhu, H.; Edvinsson, T.; Boschloo, G.; Hagfeldt, A.; Sun, L. Design of an Organic Chromophore for P-Type Dye-Sensitized Solar Cells. *Journal of the American Chemical Society* **2008**, *130*, 8570–8571, PMID: 18553967.

(26) Preat, J.; Hagfeldt, A.; Perpete, E. A. Investigation of the photoinduced electron injection processes for p-type triphenylamine-sensitized solar cells. *Energy Environ. Sci.* **2011**, *4*, 4537–4549.

(27) D'Amario, L.; Boschloo, G.; Hagfeldt, A.; Hammarström, L. Tuning of Conductivity and Density of States of NiO Mesoporous Films Used in p-Type DSSCs. *J. Phys. Chem. C* **2014**, *118*, 19556–19564.

(28) Marrani, A. G.; Novelli, V.; Sheehan, S.; Dowling, D. P.; Dini, D. Probing the Redox States at the Surface of Electroactive Nanoporous NiO Thin Films. *ACS APPLIED MATERIALS & INTERFACES* **2014**, *6*, 143–152.

(29) Renaud, A.; Chavillon, B.; Cario, L.; Le Pleux, L.; Szuwarski, N.; Pellegrin, Y.; Blart, E.; Gautron, E.; Odobel, F.; Jobic, S. Origin of the Black Color of NiO Used as Photocathode in p-Type Dye-Sensitized Solar Cells. *JOURNAL OF PHYSICAL CHEMISTRY C* **2013**, *117*, 22478–22483.